Numerical and experimental investigation of the joint stiffness in lattice structures fabricated by additive manufacturing

Guoying Dong, Yaoyao Fiona Zhao

Numerical and Experimental Investigation of the Joint Stiffness in Lattice Structures Fabricated by Additive Manufacturing

Guoying Dong, Yaoyao Fiona Zhao*

Department of Mechanical Engineering, McGill University, Montreal, Quebec, H3A 0C3, CANADA

Highlight

- A joint stiffening element is proposed to simulate lattice structures fabricated by Additive Manufacturing.
- The influence of the joint on the stiffness of the lattice structure can be considered in the proposed model.
- A parametric study is conducted to quantify the influence of the joint on a certain lattice structure and to find the optimal parameters of the joint stiffening element.
- Three-point bend testing is conducted, and it shows that the accuracy is significantly improved by the proposed model for bending dominant lattice structures.
- The computational cost of the proposed model is much lower than the tetrahedral element model.

Graphical Abstract

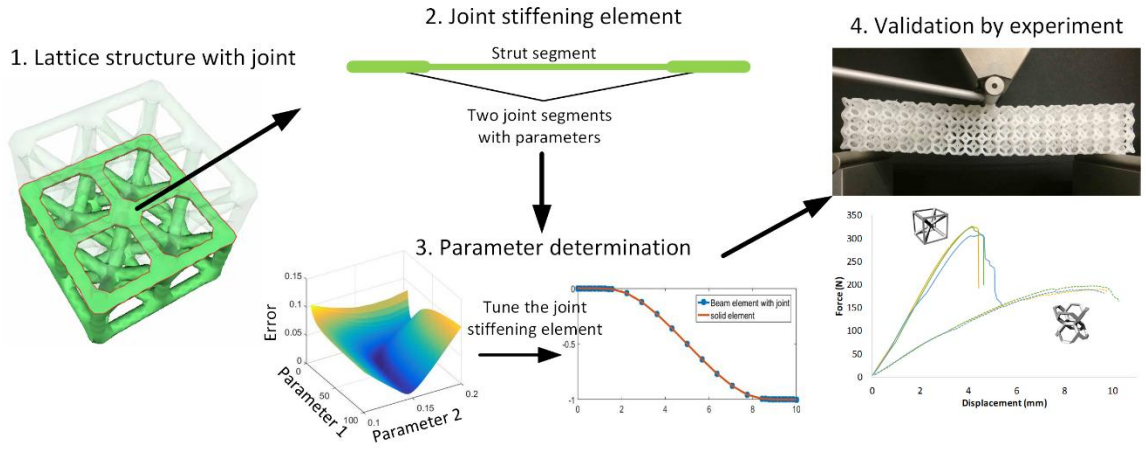

* Corresponding Author, E-mail: yaoyao.zhao@mcgill.ca

Abstract

In this paper, a concept called joint stiffening element is proposed to represent the influence of the joint on the stiffness of lattice structures fabricated by Additive Manufacturing. Four parameters are defined in the proposed element to quantify the increment of the stiffness caused by the lattice joint. Then, three-point-bend testing is used to validate the proposed model. The lattice structures with Cubic-center and Vintiles topologies are designed and fabricated for the experiment. As-fabricated material properties are obtained by tensile specimens to eliminate the influence caused by the manufacturing process and to isolate the joint stiffening effect. The result shows that models with the solid element and the proposed element are both accurate, but the proposed model has a significantly less computational cost than the solid element model. Furthermore, compared to the beam element model, the proposed model can more accurately estimate the stiffness of lattice structures, especially for the Vintiles topology. It is also found that the joint stiffening effect is more significant on the bending dominant topology than the stretching dominant topology.

Keywords: Additive Manufacturing, Finite Element Analysis, Lattice Structure, Mechanical Property

1. Introduction

The lattice structure in this paper is defined as a type of cellular architecture that has interconnected struts and joints in a three-dimensional (3D) space [1]. With the development of Additive Manufacturing (AM), the fabrication of mesoscale lattice structures has become feasible. The lattice structure can achieve unique physical properties by adjusting the distribution of materials in the design space, thus it has promising applications in the industry. The lattice structure has been widely used as a lightweight material to reduce the weight or increase the stiffness of the structure [2, 3]. It was also designed for energy absorption purpose. Tancogne-Dejean et al. [4] found that the octet lattice material featured a constant plateau stress between initial yield and densification as well as an exceptionally high specific energy absorption. Furthermore, the lattice structure has also been used for heat dissipation due to its high surface-to-volume ratio [5].

The physical properties of lattice structures have been studied for decades. In the early stage, Gibson et al. [6, 7] investigated the mechanical properties of two-dimensional (2D) and 3D cellular materials with beam theory. It was found that the effective Young's modulus was controlled by the relative density of the cellular material. After AM started to be used to fabricated lattice structures, more and more complicated lattice structures were manufactured and tested through experiments. Labeas and Sunaric [8] conducted compressive experiments to understand the static response and failure process of lattice structures made of Stainless Steel 316L. The result showed that the structural response was strongly influenced by the strut geometrical characteristics such as the aspect ratio, the unit-cell size, and the shape. Alsalla et al. [9] investigated the fracture toughness of Stainless steel 316L lattice structures through tensile tests. It was found that the result was highly influenced by the building orientation. The horizontal struts were weaker than the struts built in the vertical direction. Yang et al. [10] investigated the flexural property of auxetic lattice structures through bending tests. The result

indicated that the flexural strength of auxetic lattice structures was higher than regular sandwich panel structures. Furthermore, impact loading tests [11], dynamic tests [12], and fatigue test [13] have also been conducted to investigate the performance of lattice structures fabricated by different types of AM techniques.

Because the manufacturing cost and the time cost of most AM processes are still high, simulation methods are widely used to predict the mechanical performance of lattice structures, which accelerates the design process and saves the cost. Simulation methods are also important in the optimization process of lattice structures. Homogenization Method (HM) and Finite Element Method (FEM) are the most frequently used methods to simulate the mechanical property of lattice structures. Due to the manufacturing defects of as-build lattice structures, several methods have been used to improve the simulation method in order to more accurately predict the mechanical performance of lattice structures. Park et al. [14] proposed a two-step homogenization method considering the manufacturing influence of AM. Firstly, the effective structural element parameters were determined by a voxel-based model that included the shape deviations in the as-fabricated struts. Secondly, these parameters were implemented in the homogenization model to calculate the effective mechanical property of the lattice structure. It was found that the result obtained from the two-step approach was closer to the experimental result compared to the result from the direct homogenization method. Therefore, the shape variation caused by the manufacturing process is a crucial factor that should be considered in the simulation process. Furthermore, the manufacturing defects should also be considered in FEM. Cahill et al. [15] generated finite element models for lattice structures with both smooth surfaces and rough surfaces. The result revealed that the effective modulus of the lattice with smooth surfaces was 68% higher than that of the lattice with a rough surface. One way to improve the accuracy of the simulation result is to update the computer-aided design (CAD) model with the measurement from the fabricated sample [16]. Another way to consider the roughness of the lattice surfaces is to use beam elements [17, 18] with varying thickness to discretize the lattice strut. Furthermore, Micro-CT has been used to reconstruct the geometrical model of the as-built lattice structure. The reconstructed model can be used to generate the tetrahedral element model for FEM [19, 20].

Another aspect that needs to be considered in the simulation is the influence of the joint on the stiffness of the lattice structure. The concentration of the material in the nodal region will increase the cross-section area of the lattice strut. Labeas and Sunaric [8] increased the thickness of the beam element by 40% on 1/10 of the strut length at both strut ends to compensate for the underestimation of the stiffness. Smith et al. [21] used the same way to increase the stiffness of the strut at the joint area. Luxner et al. [22] directly increased the stiffness of the beam element at the nodal region 1000 times than the stiffness of the strut. On the contrary, Park and Rosen [23] proposed a homogenization procedure using semi-rigid joint frame elements for lattice structures. This semi-rigid joint method has been widely used in macro-scale frame structures in civil engineering [24]. They mentioned that the frame structure could not achieve a perfectly rigid joint. Therefore, the strut was modeled using semi-rigid jointed frame elements that consist of a shear deformable frame region and two joint regions at both ends. The joints were modeled as point-connections in conventional frame elements. The

elastic modulus obtained by the proposed model is less than the conventional frame model, which means the actual stiffness of the lattice structure was reduced by the joints.

Even though the influence of the joint of the stiffness of lattice structures has been considered in previous studies. It is not clear how much the joint will affect the stiffness of the strut. In this paper, the stiffness of the joint in the lattice structure will be investigated quantitatively. Then, a joint stiffening element is proposed to precisely estimate the influence of the joint on the stiffness of lattice structures. It can be used to build FEM models to simulate the mechanical performance of entire lattice structures. In Section 2, the influence of the joint on the stiffness is discussed first. Then, a joint stiffening element is proposed to model the lattice strut with the influence of joints. In Section 3, a parametric study is carried out to find the optimal coefficients for the joint stiffening element. A case study is presented in Section 4 to demonstrate the process of simulating lattice structures with the joint stiffening element. The as-fabricated material property is obtained by tensile specimens to eliminate the imperfection caused in the manufacturing process. The result from the proposed simulation model and the traditional models are compared with the experimental result. Finally, the conclusions and future research are summarized in Section 5.

2. The proposed joint stiffening element

2.1 Effects of joints on the stiffness of lattice structures

The joint in the lattice structure has the influence on the structural stiffness for two reasons. The first reason is that the size of the joint in the CAD model is relatively large compared to the strut thickness. The second reason is that the material tends to concentrate in the joint area during the fabrication by AM. In this paper, only the joint geometry designed by the CAD model is considered. A comparison of the joint sizes of two lattice structures is shown in Figure 1. The joint in Figure 1(a) is only the intersection of the cylindrical struts. But in Figure 1(b), there is a large joint used to connect the surrounding struts. In the geometrical modeling process of the lattice structure, there are lots of struts that need to be connected by the Boolean operation. Generally, joints are used to trim the intersection of lattice struts so that the difficulty of the Boolean operation can be reduced. However, it makes the joint size larger than the thickness of the strut. For the bending dominant lattice topologies, the stress will concentrate at the end of the strut. The large joint will affect the stiffness at the end of the strut. If the beam element is used to simulation the mechanical performance of the lattice structure, the total stiffness of the structure tends to be underestimated. Because in the traditional beam element model, the stiffness is uniform on the beam element.

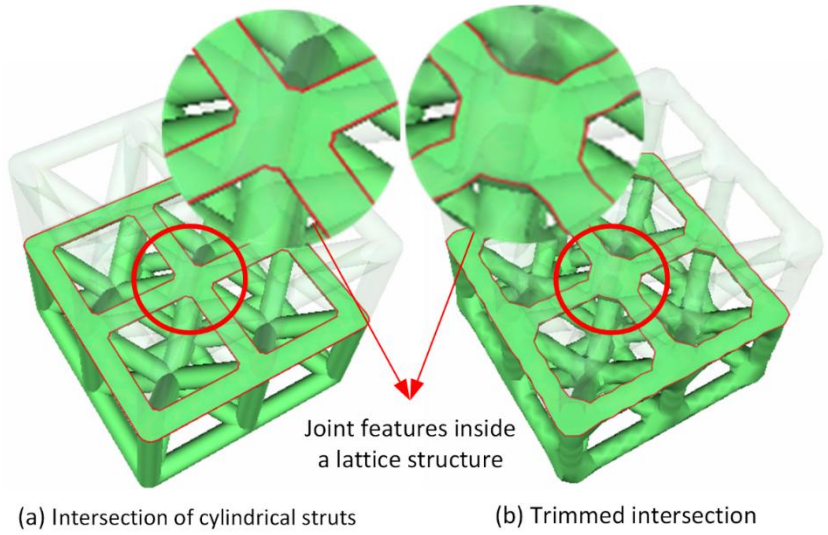

Figure 1 The comparison of the joint sizes with different types of intersection

A unit cell of Vintiles lattice structure is simulated by both the solid element model and the beam element model to investigate the stiffness underestimation. The solid element is generated by the CAD model of the lattice structure. The geometry of the joints and the lattice struts are both meshed with the tetrahedral element. Therefore, in the solid element model, the influence of the joint on the stiffness of the lattice structure is considered. However, the beam element model uses Timoshenko beam elements to mesh the wireframe of the lattice structure. All the beam elements have the uniform thickness. The geometry of the joint is not considered in the beam element model. Some parameters of both simulation models are summarized in Table 1. Convergence tests are conducted for both the solid element model and the beam element model as shown in Figure 2. It is found that if the number of the solid element is small, the result is 42.5% higher than the converged result. Therefore, a large number of elements is required for an accurate simulation result of the 3D solid element model. However, when the lattice structure has a lot of unit cells, it will be extremely difficult to generate the 3D mesh of the structure. The meshing algorithm of the commercial software may fail in the mesh generation. This is one reason that the beam element model is preferred to simulate complicated lattice structure. The comparison of the converged simulation results is shown in Figure 2(c). The total CPU time of the solid element model is 19.2s (119754 elements) while that of the beam element model is 0.3s (720 elements). However, it should be noted that this is only a single unit cell. If the lattice structure has plenty of unit cells, the computational cost of the solid element model will be significantly high. For example, if the lattice structure has 10 unit cells along each axis, the total CPU time of the solid element will be more than 5 hours. But the time of the beam element model will be only 5 minutes. Therefore, beam element is the ideal element type to simulate complex lattice structures. The current problem of the beam element is that the stiffness of joints in the lattice structure is underestimated. It can be seen from Figure 2(c) that under the same loading condition, the effective elastic modulus of the solid element model is 1755MPa while that of the beam element model is only 1133MPa. This proves that the stiffness of the beam element model is much lower than that of the solid element model.

Therefore, the beam element model should be modified so that the influence of the joint can be considered in the simulation process.

Table 1 The parameters in the simulation models

Topology	Cell size	Number of cells on each axis	Strut thickness	Young's modulus	Poisson's ratio
Vintiles	50mm	1	8mm	150GPa	0.3

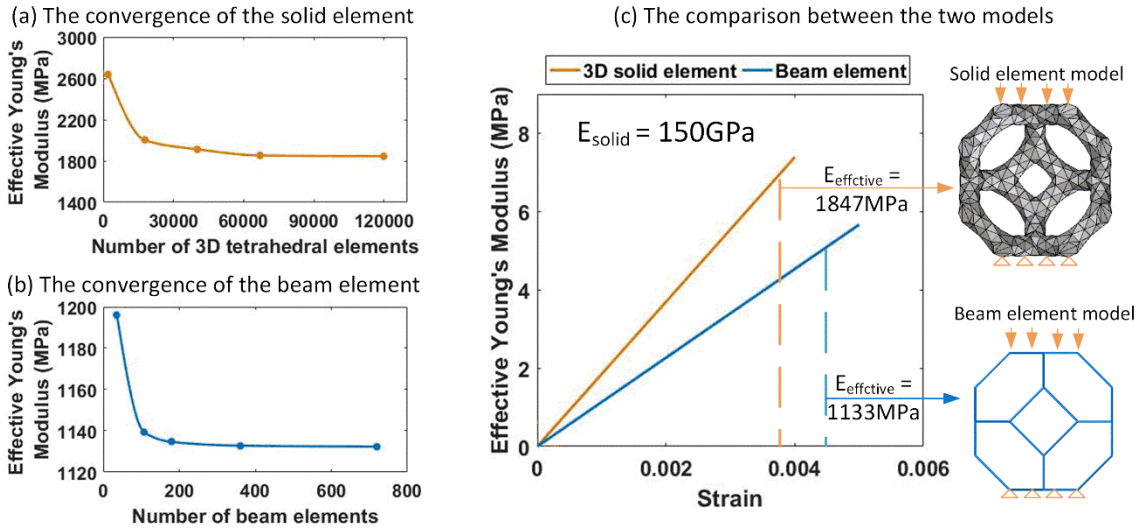

Figure 2 The simulation results with the convergence test to show the influence of the joint

2.2 The proposed concept of the Joint stiffening element

To consider the joint stiffening effect on the lattice structure, a joint stiffening element is proposed. It is modified from the Timoshenko beam element. The conceptual configuration of the joint stiffening element is shown in Figure 3. The joint stiffening element consists of three segments. Two segments at the end of the element represent the joint area in the lattice structure. The middle segment of the joint stiffening element represents the actual length of the lattice strut. L_j and L_s are the length of the joint stiffening segment and the strut segment, respectively. w_1, w_2 and ϕ_1, ϕ_2 are the deflections and the rotations at two ends of the element. $\overline{w}_1, \overline{w}_2$ and $\bar{\phi}_1, \bar{\phi}_2$ are the deflections and the rotations at the internal nodes of the element. Because the cross-section of the joint has a larger area than that of the lattice strut, the flexural stiffness of the joint is greater than the flexural stiffness of the strut. Therefore, a flexural coefficient C_f is proposed to compensate for the stiffness of the joint.

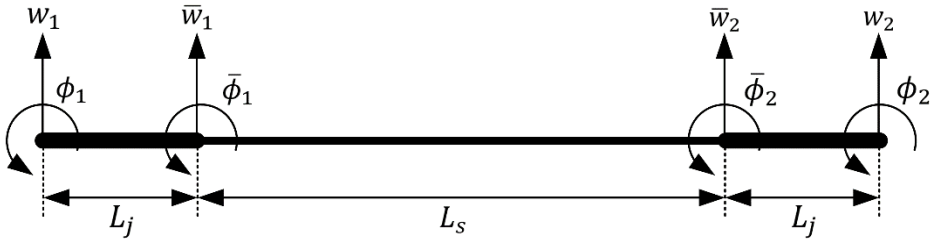

Figure 3 The conceptual configuration of the joint stiffening element.

The force-displacement equation for the Timoshenko beam element is derived from the method in the literature [25]:

$$[\mathbf{K}_e][\mathbf{u}_e] = [\mathbf{f}_e] \tag{1}$$

$$[\mathbf{K}_e] = \left(\frac{2EI}{\mu_e h_e^3}\right)\begin{bmatrix} 6 & -3h_e & -6 & -3h_e \\ -3h_e & 2h_e^2\Sigma_e & 3h_e & h_e^2\Theta_e \\ -6 & 3h_e & 6 & 3h_e \\ -3h_e & h_e^2\Theta_e & 3h_e & 2h_e^2\Sigma_e \end{bmatrix} \tag{2}$$

$$\Lambda_e = \frac{EI}{GAK_s h_e^2} \quad \mu_e = 1 + 12\Lambda_e \quad \Theta_e = 1 - 6\Lambda_e \quad \Sigma_e = 1 + 3\Lambda_e \tag{3}$$

$$[\mathbf{u}_e] = [w_a, \phi_a, w_b, \phi_b]^T \tag{4}$$

$$[\mathbf{f}_e] = [V_a, M_a, V_b, M_b]^T \tag{5}$$

where E is the Young's modulus, G is the shear modulus, A is the area of the strut cross section, I is the moment of inertia, K_s is the shear correction coefficient, and h_e is the length of the beam element. $[\mathbf{K}_e]$ is the stiffness matrix of the Timoshenko beam element. $[\mathbf{u}_e]$ is the flexural displacement and the rotation on the nodes, and $[\mathbf{f}_e]$ is the transverse force and moment on the end nodes of the beam element.

To represent the length of the joint segment and the strut segment, a joint length coefficient C_l is proposed. L_j and L_s can be calculated as:

$$L_j = LC_l \tag{6}$$

$$L_s = L(1 - 2C_l) \tag{7}$$

where L is the total length of the joint stiffening element. By substituting L_j and L_s into Eq. (2), the stiffness matrices of the joint segment and the strut segment can be obtained as:

$$\left[\mathbf{K}_j\right] = C_f[\mathbf{K}_e]\left(\text{let } h_e = L_j\right) \tag{8}$$

$$[\mathbf{K}_s] = [\mathbf{K}_e]\,(\text{let } h_e = L_s) \tag{9}$$

The stiffness matrix of the joint segment is multiplied by C_f so that the stiffening effect of the joint can be considered in the simulation of lattice structures. The global stiffness matrix can be assembled from $\left[\mathbf{K}_j\right]$ and $[\mathbf{K}_s]$. The total force-displacement equation for the joint stiffening element can be written as

$$\begin{bmatrix} K_j^{(11)} & K_j^{(12)} & K_j^{(13)} & K_j^{(14)} & 0 & 0 & 0 & 0 \\ K_j^{(21)} & K_j^{(22)} & K_j^{(23)} & K_j^{(24)} & 0 & 0 & 0 & 0 \\ K_j^{(31)} & K_j^{(32)} & K_j^{(33)}+K_s^{(11)} & K_j^{(34)}+K_s^{(12)} & K_s^{(13)} & K_s^{(14)} & 0 & 0 \\ K_j^{(41)} & K_j^{(42)} & K_j^{(43)}+K_s^{(21)} & K_j^{(44)}+K_s^{(22)} & K_s^{(23)} & K_s^{(24)} & 0 & 0 \\ 0 & 0 & K_s^{(31)} & K_s^{(32)} & K_j^{(11)}+K_s^{(33)} & K_j^{(12)}+K_s^{(34)} & K_j^{(13)} & K_j^{(14)} \\ 0 & 0 & K_s^{(41)} & K_s^{(42)} & K_j^{(21)}+K_s^{(43)} & K_j^{(22)}+K_s^{(44)} & K_j^{(23)} & K_j^{(24)} \\ 0 & 0 & 0 & 0 & K_j^{(31)} & K_j^{(32)} & K_j^{(33)} & K_j^{(34)} \\ 0 & 0 & 0 & 0 & K_j^{(41)} & K_j^{(42)} & K_j^{(43)} & K_j^{(44)} \end{bmatrix} \begin{bmatrix} w_1 \\ \phi_1 \\ \bar{w}_1 \\ \bar{\phi}_1 \\ \bar{w}_2 \\ \bar{\phi}_2 \\ w_2 \\ \phi_2 \end{bmatrix} = \begin{bmatrix} V_1 \\ M_1 \\ \bar{V}_1 \\ \bar{M}_1 \\ \bar{V}_2 \\ \bar{M}_2 \\ V_2 \\ M_2 \end{bmatrix} \tag{10}$$

Since the degrees of freedom at the second node and the third node do not correspond to a degree of freedom of any other element, they can be eliminated to obtain the element stiffness matrix that corresponds to the degrees of freedom at the first and fourth nodes only. Static condensation is employed to reduce the number of element degrees of freedom [26, 27]. The elimination of the degrees of freedom at the second and third nodes is carried out using Gauss elimination. Eq. (10) can be partitioned as:

$$\begin{bmatrix} K_j^{(31)} & K_j^{(32)} & 0 & 0 \\ K_j^{(41)} & K_j^{(42)} & 0 & 0 \\ 0 & 0 & K_j^{(13)} & K_j^{(14)} \\ 0 & 0 & K_j^{(23)} & K_j^{(24)} \end{bmatrix} \begin{bmatrix} w_1 \\ \phi_1 \\ w_2 \\ \phi_2 \end{bmatrix} + \begin{bmatrix} K_j^{(33)}+K_s^{(11)} & K_j^{(34)}+K_s^{(12)} & K_s^{(13)} & K_s^{(14)} \\ K_j^{(43)}+K_s^{(21)} & K_j^{(44)}+K_s^{(22)} & K_s^{(23)} & K_s^{(24)} \\ K_s^{(31)} & K_s^{(32)} & K_j^{(11)}+K_s^{(33)} & K_j^{(12)}+K_s^{(34)} \\ K_s^{(41)} & K_s^{(42)} & K_j^{(21)}+K_s^{(43)} & K_j^{(22)}+K_s^{(44)} \end{bmatrix} \begin{bmatrix} \bar{w}_1 \\ \bar{\phi}_1 \\ \bar{w}_2 \\ \bar{\phi}_2 \end{bmatrix} = \begin{bmatrix} 0 \\ 0 \\ 0 \\ 0 \end{bmatrix} \tag{11}$$

$$\begin{bmatrix} K_j^{(11)} & K_j^{(12)} & 0 & 0 \\ K_j^{(21)} & K_j^{(22)} & 0 & 0 \\ 0 & 0 & K_j^{(33)} & K_j^{(34)} \\ 0 & 0 & K_j^{(43)} & K_j^{(44)} \end{bmatrix} \begin{bmatrix} w_1 \\ \phi_1 \\ w_2 \\ \phi_2 \end{bmatrix} + \begin{bmatrix} K_j^{(13)} & K_j^{(14)} & 0 & 0 \\ K_j^{(23)} & K_j^{(24)} & 0 & 0 \\ 0 & 0 & K_j^{(31)} & K_j^{(32)} \\ 0 & 0 & K_j^{(41)} & K_j^{(42)} \end{bmatrix} \begin{bmatrix} \bar{w}_1 \\ \bar{\phi}_1 \\ \bar{w}_2 \\ \bar{\phi}_2 \end{bmatrix} = \begin{bmatrix} V_1 \\ M_1 \\ V_2 \\ M_2 \end{bmatrix} \tag{12}$$

For simplicity, Eq. (11) and Eq. (12) can be written as:

$$[\mathbf{K1}][\mathbf{U}_f] + [\mathbf{K2}][\bar{\mathbf{U}}_f] = [\mathbf{0}] \tag{13}$$

$$[\mathbf{K3}][\mathbf{U}_f] + [\mathbf{K4}][\bar{\mathbf{U}}_f] = [\mathbf{F}_f] \tag{14}$$

The internal displacement and rotation can be calculated as:

$$\left[\bar{\mathbf{U}}_f\right] = -[\mathbf{K2}]^{-1}[\mathbf{K1}][\mathbf{U}_f] \tag{15}$$

By substituting Eq. (15) into Eq. (14), the total force-displacement equation can be written as:

$$[\mathbf{K}_f]\left[\mathbf{U}_f\right] = [\mathbf{F}_f] \tag{16}$$

where

$$\left[\mathbf{K}_f\right] = [\mathbf{K3}] - [\mathbf{K4}][\mathbf{K2}]^{-1}[\mathbf{K1}] \tag{17}$$

The four-nodes joint stiffening element can be condensed into a two-node element by Eq. (17). $\left[\mathbf{K}_f\right]$ is the flexural stiffness matrix of the joint stiffening element. There are two parameters C_f and C_l that control the joint property. The stiffness coefficient C_f determines the amplification factor of the flexural stiffness at the joint. The length coefficient C_l indicates the length of the joint area compared to the total length of the strut. The calculation of C_f and C_l will be discussed in Section 3.

Apart from the flexural stiffness, the axial stiffness of the lattice strut is also influenced by the joint in the lattice structure. The axial stiffness matrix of the joint stiffening element is derived as:

$$[\mathbf{K}_{axial}] = \begin{bmatrix} k_a & -k_a \\ -k_a & k_a \end{bmatrix} \tag{18}$$

$$\frac{1}{k_a} = \frac{1}{k_a^j} + \frac{1}{k_a^s} + \frac{1}{k_a^j} \tag{19}$$

$$k_a^j = \frac{C_a EA}{L_{j,a}} \quad k_a^s = \frac{EA}{L_{s,a}} \tag{20}$$

where

$$L_{j,a} = LC_{l,a} \tag{21}$$

$$L_{s,a} = L(1 - 2C_{l,a}) \tag{22}$$

where $C_{l,a}$ is the length coefficient for the joint segment under the axial load, C_a is the axial stiffness coefficient of the joint segment. Because the formulation of the axial stiffness matrix is not related to the moment of inertia, which is different from the flexural stiffness matrix. The influence of the joint on the axial part and the flexural part are different. Therefore, new parameters $C_{l,a}$ and C_a are used for the axial stiffness matrix.

Similar to the axial stiffness matrix, the torsional stiffness matrix of the joint stiffening element is derived as:

$$[\mathbf{K}_{torsion}] = \begin{bmatrix} k_t & -k_t \\ -k_t & k_t \end{bmatrix} \tag{23}$$

$$\frac{1}{k_t} = \frac{1}{k_t^j} + \frac{1}{k_t^s} + \frac{1}{k_t^j} \tag{24}$$

$$k_t^j = \frac{C_f GJ}{L_j} \quad k_t^s = \frac{GJ}{L_s} \tag{25}$$

where J is the torsion constant. Because both the moment of inertia I and the torsion constant J are proportional to the fourth power of the strut radius. The influence of the joint on the flexural stiffness and the torsional stiffness are similar. Therefore, the length coefficient and the stiffness coefficient for the flexural load and the torsional load are the same. The total force-displacement equation can be assembled from Eq. (16), Eq. (18), and Eq. (23) as:

$$[\mathbf{K}_{total}]_{(12\times12)}[\mathbf{U}]_{(12\times1)} = [\mathbf{F}]_{(12\times1)} \tag{26}$$

3. Calculation of parameters

In the proposed joint stiffening element model, there are four coefficients evaluating the influence of the joint. They are the flexural stiffness coefficient C_f; the axial stiffness coefficient C_a; the length coefficient C_l and $C_{l,a}$. The determination of these parameters will be introduced in this section. The first step is to quantify the influence of the joint on the mechanical performance of the lattice strut by the tetrahedral element model. A convergence test is conducted to ensure the accuracy of the result. Secondly, the joint stiffening element model of

the lattice strut is used to obtain a group of results with a range of parameters. Finally, one pair of parameters in the joint stiffening element model will be selected whose result is closest to the result in the tetrahedral element model.

3.1 Tetrahedral element model of the lattice strut

In order to get the tetrahedral element model of lattice strut, one lattice strut is cut from the lattice structure as shown in Figure 4. Other lattice struts connected to the joint are removed so that only one strut is left with joints at the two ends. The single lattice strut model is then meshed by 4-node tetrahedral elements. Different mesh sizes are used to generate multiple models for the convergence test. Because only a single strut is simulated, the computational cost is acceptable when the result converges. Examples of the numerical model are shown in Figure 5. Both numerical models are fixed at the left end. The numerical model in Figure 5(a) is forced with a unit transverse displacement to simulate the flexural behavior of the lattice strut. The numerical model in Figure 5(b) is forced with a unit axial displacement to simulation the tensile behavior of the lattice strut. To indicate the influence of the joint on the stiffness of the lattice strut, two beam element models are also generated with the same boundary condition as that in tetrahedral element models.

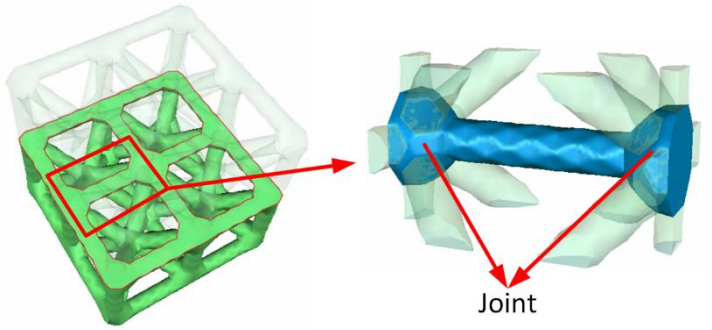

Figure 4 The geometrical model of the joint stiffening element inside a lattice structure.

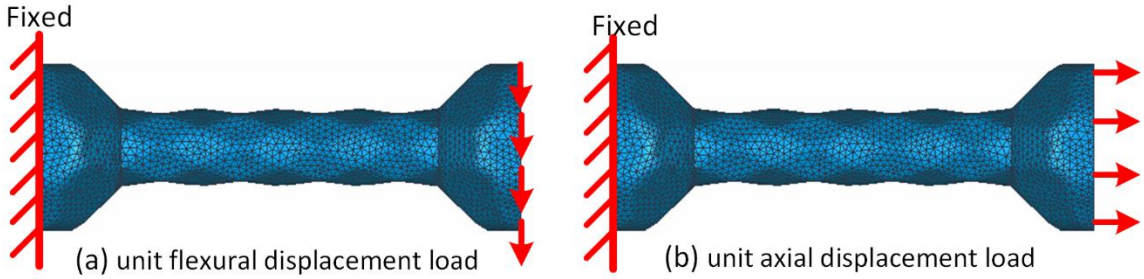

Figure 5 Numerical model and the boundary conditions of the single lattice strut.

The simulation results of the tetrahedral element models and the beam element models are shown in Figure 6. The total length of the strut in the simulation is 10. The relationship between the displacement and the axial position are demonstrated by the curves in Figure 6. It is found that there is a significant difference between the solid element model and the beam element model. The slope of the red curve is smaller than that of the blue curve at the two ends of the strut. This is because the stiffness at the two ends of the strut is much higher than the middle of

the strut. The deformation should concentrate in the middle of the strut. The solid element model can reflect the actual stiffness of the joint while the beam element model does not consider the joint. Therefore, the strut is very strong at both ends in the solid element model. It causes the deformation at the ends of red curves (solid element model) smaller than that in the blue curves (beam element model).

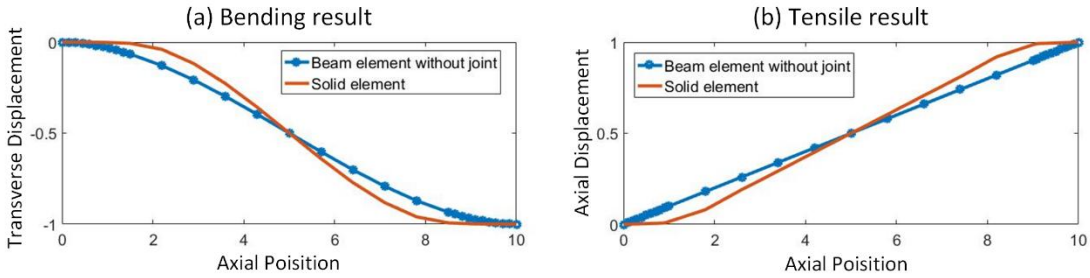

Figure 6 Comparison of the simulation results of the solid element model and the beam element model without considering the joint stiffening effect.

3.2 Determination of the optimal parameters

The comparison of the results in Figure 6 shows that the stiffness at the end of the beam element should be increased to match the actual stiffness of the joint. The next step is to determine the stiffness and the length coefficients of the joint stiffening element. Firstly, a range of coefficients is selected to generate the joint stiffening element model of the lattice strut. Then, a group of results can be obtained from the joint stiffening element models. To evaluate the accuracy of selected coefficients, n points with position x_i $(\mathrm{i} = 1 \dots \mathrm{n})$ on the lattice strut will be chosen. The error between the solid element model and the joint stiffening element model is calculated by

$$\mathrm{e} = \sum_{i=1}^{n} \left\| u_s(x_i) - u_j(x_i) \right\|_2 \tag{27}$$

where $u_s(x_i)$ is displacement of the solid element model at the position x_i, $u_j(x_i)$ is the displacement of the joint stiffening element model. If the error is small, it means the result of the joint stiffening element is close to the solid element result.

A series of stiffness and length coefficients are generated for the flexural load and the axial load. Each combination of the stiffness and length coefficients has been used to calculate the deformation of the lattice strut. Then, the error between the solid element model and the joint stiffening element model are calculated from Eq. (27). The relationships between the error and the coefficients are shown in Figure 7. In this example, C_f is from 1 to 100, C_l is from 0.1 to 0.2, C_a is from 1 to 20, and $C_{l,a}$ is from 0.05 to 0.2. Each parameter has 50 items within its range. When the combination of the stiffness coefficient and the length coefficient gives the minimum error, they will be selected as the optimal parameters for the joint stiffening element.

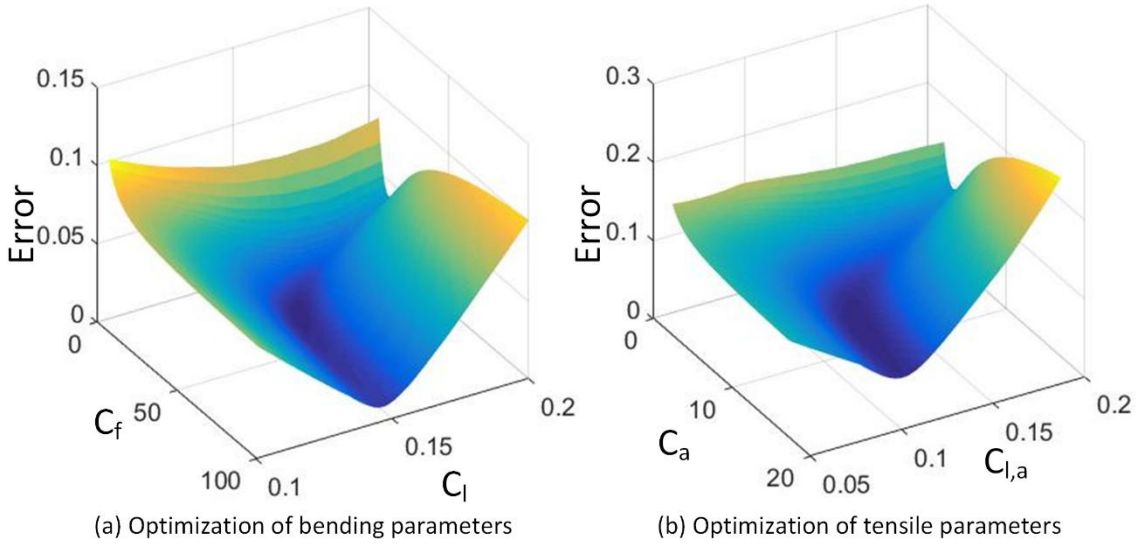

Figure 7 The relationship between the error and the coefficients

3.3 Validation of selected parameters

After the determination of the optimal coefficients, these coefficients are imported into the joint stiffening element. The result of the optimized joint stiffening element is compared to the solid element model as shown in Figure 8. It is found that the results of both models coincide, which means the displacement in the joint stiffening element is nearly the same as the displacement of the solid element model. Therefore, the joint stiffening element can accurately reflect the influence of the joint on the stiffness of the lattice strut. Because the beam element does not consider the influence of the joint, it underestimates the stiffness of the lattice structure. It is more accurate to simulate the lattice structure with the proposed model than using the beam element model alone.

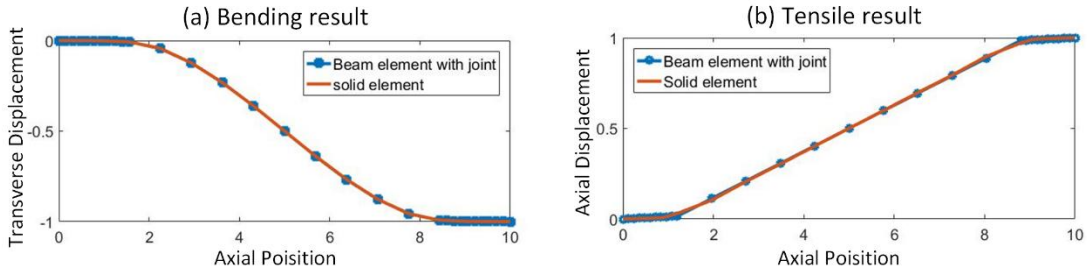

Figure 8 The comparison of the optimized joint stiffening element result and the solid element result

4. Case study

To validate the proposed joint stiffening element, two lattice structures with the Cubic-center topology and the Vintiles topology are designed for the three-point-bend testing as shown in Figure 9. Both lattice structures have $18 \times 3 \times 3$ cells along x, y, and z-direction. The dimension of the unit cell is 10mm in all three axes. The relative density of both structures is 15%. The Cubic-center topology is stretching dominant while the Vintiles topology is bending dominant. It is assumed that the joint will have more influence on the bending dominant topology than that

of the stretching dominant topology. Because the stress is concentrated at the end of the beam element if it is under bending load. The underestimation of the joint stiffness will be magnified by the stress concentration. This assumption will also be validated in this case study.

4.1 As-fabricated material property

The lattice structures are fabricated by Fused Deposition Modeling (FDM) process with ABS materials. In order to obtain the bulk material properties more accurately, several tensile parts are designed as shown in Figure 9(c). Two specimens are designed so that the testing strut can be put parallel, inclined, and perpendicular to the build platform. The lattice samples and the tensile specimens are fabricated together in one batch as shown in Figure 10(a). The as-fabricated samples are shown in Figure 10(b). Because there are several factors in the FDM process, such as the toolpath and the layer adhesion that may have the influence on the material property. The as-fabricated material tends to be different from the bulk material. The influence from the manufacturing process should be eliminated as much as possible so that the joint stiffening effect can be isolated. Otherwise, the manufacturing influence may reduce the stiffness of the lattice structure, which may counteract the joint stiffening effect and lead to wrong results. Therefore, the tensile specimens are designed with struts that have the diameter close to the strut thickness in the lattice structure. All the parameters used in the fabrication are the same for both the tensile specimen and the lattice structure. The tool path in the lattice strut is similar to the tool path in the specimen. The strength of the adhesion between layers can be investigated by the vertical specimen.

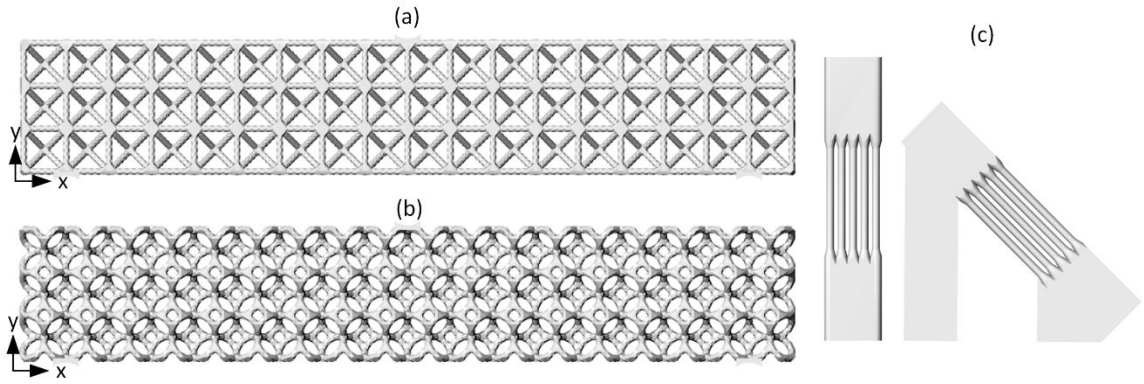

Figure 9 The geometrical model of the three-point bend testing, (a) Cubic-center lattice structure, (b) Vintiles lattice structure, and (c) tensile specimens used to obtain the elastic modulus of the bulk material.

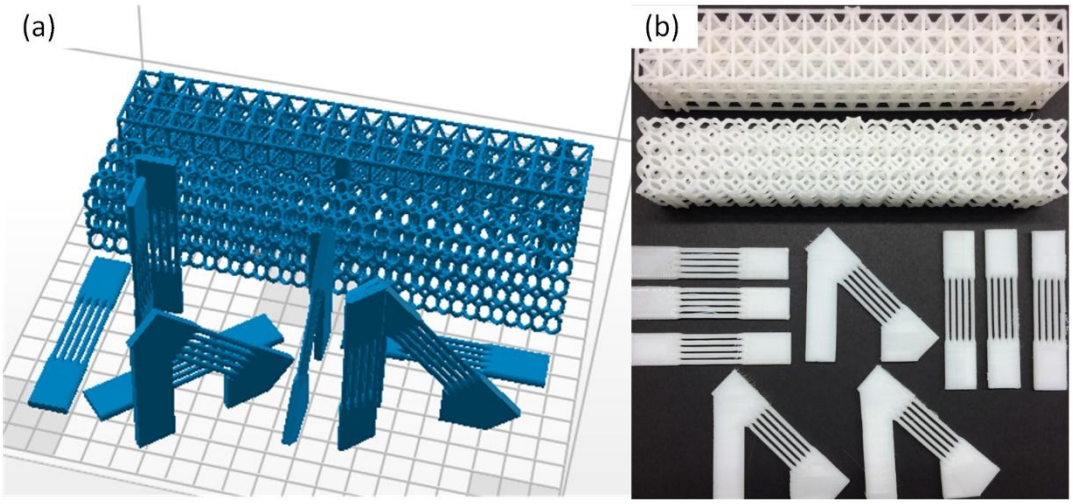

Figure 10 (a) Printing set-up for the lattice structures and the tensile specimens. (b) as-built samples.

The strain rate of the tensile test is 1mm/min. The load cell is 5kN. A strain gauge is used to measure the strain of the specimen. The averaged testing results and the standard deviations of the tensile samples are shown in Figure 11. It is found that the elastic modulus of the horizontal specimen and the inclined specimen are very close. But the elastic modulus of the vertical specimen is 20% lower than the other two specimens. It is concluded that the adhesion between layers will reduce the elastic modulus of as-fabricated parts. Then, the as-fabricated material property will be imported into the simulation model. The lattice strut with different orientation will be assigned with different properties. This can minimize the inaccuracy that comes from the material property. The elastic modulus and the flexural modulus are also tested by ASTM D638 [28] and ASTM D790 [29] for comparison as shown in Figure 11. Because the tool path has influence on the mechanical property of the FDM fabricated parts, the elastic modulus of these samples is different. Only the proposed test samples have the same tool path with that of the lattice strut. It is more reasonable to use the elastic modulus of the proposed tensile specimens in the simulation process.

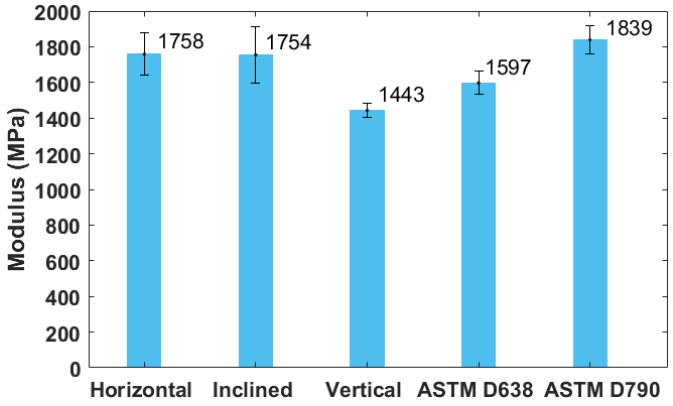

Figure 11 The elastic modulus of the tensile specimens and the flexural modulus of the bending specimens.

4.2 Determination of optimal coefficients

The next step is to determine the coefficients for the joint stiffening element models of both lattice structures. Firstly, the strut models of these two lattice structures are generated with tetrahedral elements similar to the models shown in Figure 5. The unit flexural displacement load and the unit axial displacement load are applied to the strut models. Secondly, a series of flexural coefficients and axial coefficients are imported into the joint stiffening element models. Then, Eq. (27) is used to calculate the error between the tetrahedral element model and the joint stiffening element model. When the error gets the minimum value, the corresponding coefficients are selected as the optimal parameters. The optimal coefficients for the flexural load and the axial load are summarized in Table 2.

Table 2 Optimal coefficients for the designed lattice structures

	Flexural coefficient		Axial coefficient	
	C_f	C_l	C_a	$C_{l,a}$
Cubic-center	31.5	0.155	2.16	0.162
Vintiles	4.6	0.213	2.36	0.183

The optimal coefficients are used in the joint stiffening element model to simulate the three-point bending performance of the designed lattice structures. To compare the result of the proposed models, the designed lattice structures are also meshed by Timoshenko beam elements and tetrahedral elements. The Timoshenko beam element model is generated by the lattice wireframe, which means it doesn't consider the influence of the joint on the stiffness of the structure. By contrast, the tetrahedral element is generated based on the geometrical model of the lattice structure, which takes the joints into consideration.

4.3 Results and Discussion

Physical tests are used to validate the simulation results. The three-point-bend testing is conducted on the TestResources 313 universal tester as shown in Figure 12. The load-displacement curves of both lattice structures are shown in Figure 13. Each of them is fabricated and tested three times to reduce the uncertainty of the FDM machine. The average stiffness and the standard deviation of stiffness is calculated for both lattice structures. It can be found in the experiment that the stretching dominant lattice structure tends to exhibit a higher stiffness than the bending dominant lattice when they have the same relative density. But deformation of the stretching dominant lattice at the ultimate load is smaller than that of the bending dominant lattice. The load-displacement curves in Figure 13 show that the Cubic-center lattice structure fails earlier than the Vintiles lattice structure. This is because the Cubic-center topology is stretching dominant while the Vintiles topology is bending dominant. The load on the strut of stretching dominant lattices is mainly the axial force. But in the bending dominant lattice structure, most of the struts are under flexural load.

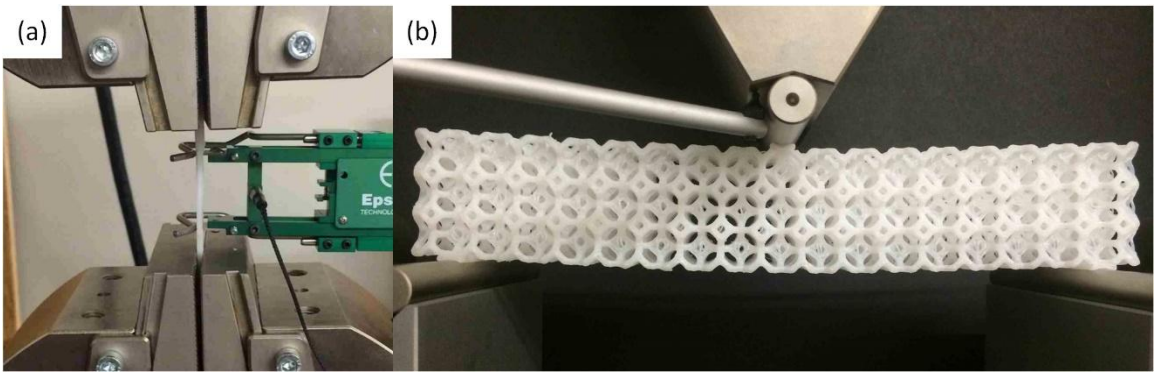

Figure 12 Mechanical test on (a) the tensile specimen and (b) the three-point bending lattice structure.

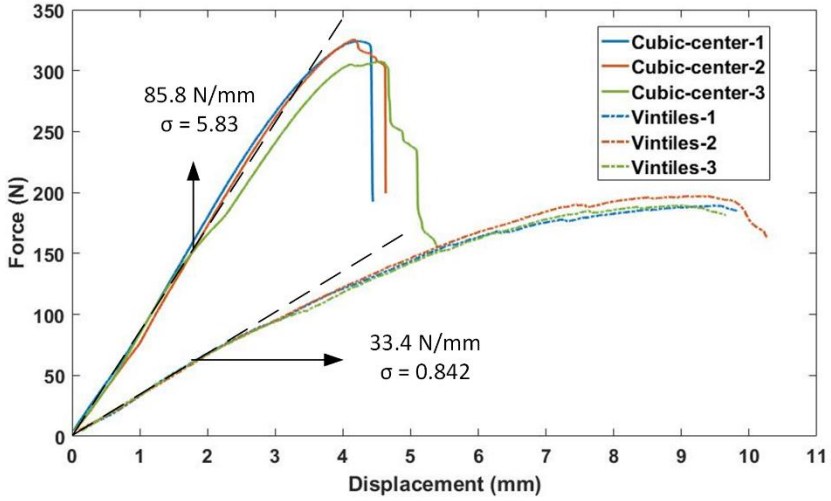

Figure 13 The load-displacement curves of the Cubic-center and Vintiles lattice structures, σ is the standard deviation of the stiffness

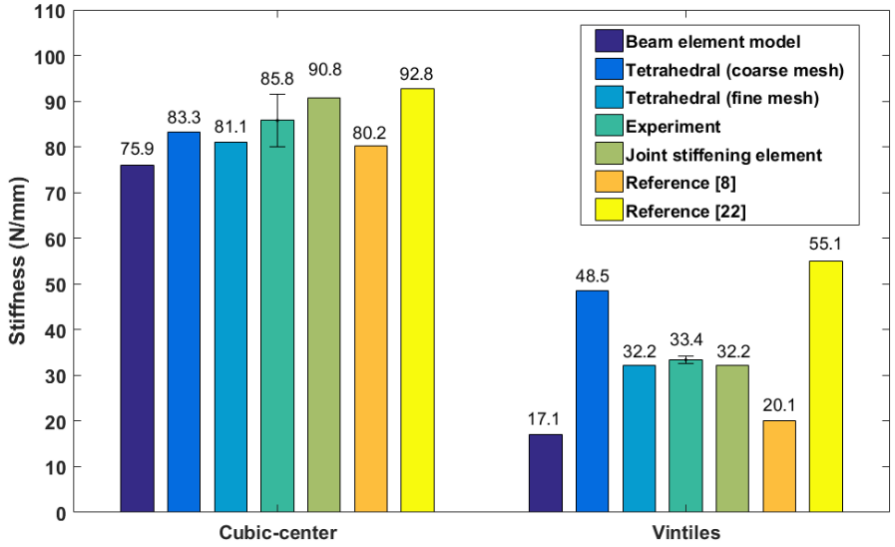

Figure 14 The stiffness of the lattice structure under the three-point bending load obtained from the simulation and experiment, the error bar represents the standard deviation of the experimental result

In order to compare experimental results with simulation results, the average stiffness and the standard deviation of the as-fabricated lattice structure is calculated from the load-displacement curves. The results of the stiffness obtained by both the simulation method and the experimental method are summarized in Figure 14. The tetrahedral mesh in the simulation model is generated by Altair HyperWorks. All the simulation models except the proposed model are solved by Abaqus. Four-node tetrahedral element (C3D4) is used in the solid element model. Two-node beam element (B31) is used in the beam element model and the models in the literature. A self-contained beam element solver is written in Matlab to solve the proposed model. The parameters used in the joint stiffening element are integrated into the Matlab code. The parameters in Table 2 are the inputs of the Matlab code.

For the Cubic-center lattice structure, the difference between the beam element model and the solid element model is relatively small. However, the stiffness of the Vintiles lattice structure predicted by the beam element model is much lower than that predicted by the solid element model. It means that the joint stiffening effect is more obvious on the bending dominant topology than the stretching dominant topology. It can be explained by the formulation of the stiffness matrix of the beam element. The bending part of the stiffness matrix includes the moment of inertia, which is proportional to the fourth square of the radius. The axial part of the stiffness only includes the cross-section area, which is proportional to the square of the radius. If the radius at the joint area is increased, the bending part is more positively influenced. The deformation of the struts in Vintiles lattice is mainly contributed by the bending deformation. But the deformation of the struts in Cubic-center lattice is mainly contributed by the axial deformation. Therefore, the Vintiles lattice structure is more positively influenced by the joint. The second reason is that the stress in the strut of Vintiles lattice concentrates at the joint area. But the stress is more uniformly distributed in the strut of Cubic-center lattice structure. Since the cross-section area of the joint is larger than that of the strut. It can be considered as adding materials in the stress concentration area. Therefore, it has more influence on the stiffness of the Vintiles lattice structure.

The result also shows that the joint stiffening element model can increase the estimated stiffness compared to the beam element model. The result of the Vintiles lattice structure is doubled when the stiffness of the joint is considered in the proposed model. Furthermore, it is found that, compared to the results of the beam element and tetrahedral element models, the results in the proposed model are closer to the experimental results for both topologies, especially for the Vintiles topology. It can be concluded that the proposed model is able to predict the mechanical performance of lattice structures more accurately. The joint stiffening effect must be considered in bending dominant topologies. Otherwise, the stiffness of the structure will be seriously underestimated by the beam element model.

The proposed model is also compared to existing methods in the literature that consider the increase of the joint stiffness as shown in Figure 14. One method is that 1/10 of the strut at the end are modeled with a 40% higher cross-section area [8]. Another method is to increase the stiffness of the beam element 1000 times inside a sphere centered at the joint that has the same radius as the strut [22]. Even though these two methods can improve the stiffness of the lattice structure, they have a large deviation from the experimental result. It is found that the first method underestimates the stiffness while the second method overestimates the stiffness.

This is because the parameters in their methods are determined by experience. But the proposed model has a systemic method to optimize parameters used in the joint stiffening element, which lead to a more accurate result in the proposed model. Furthermore, both models in the literature require a larger quantity of the beam element than the proposed model. The quantity of mesh is around 10 times than the proposed model.

The advantage of the proposed model compared to the solid element model is that the computational cost of the proposed model is much lower than the solid element model. Because the geometry of the lattice structure is very complicated with a lot of small features. It will lead to much difficulty in the generation of the 3D tetrahedron mesh. The size of each tetrahedron element needs to be very small to improve the mesh quality, which means the total number of the element is very large. It can be found in Figure 14 that the coarse tetrahedral mesh model of the Vintiles lattice structure does not obtain an accurate result. Even though the accuracy of the solid element model of the Vintiles lattice structure can be improved by using a finer mesh. The computational cost is much higher than that of the other simulation models. The comparison of the quantity of the mesh between the solid element model and the proposed element model is shown in Table 3. A large number of meshes means the degrees of freedom of the structure is high. It takes more memory and time to solve the linear system of the structure. Instead, the beam element can mesh the lattice structure by using the wireframe information. Each lattice strut can be modeled with one beam element. This will significantly reduce the computational cost in the simulation of the mechanical performance of lattice structures. The computational time to solve the proposed model and solid element models are also summarized in Table 3. The fine mesh model takes around one hour to solve the FEA equations while the proposed model only takes a second. It should be noted that the time of the meshing process has not been included yet. The time to generate the 3D solid element is also much longer than that to generate the joint stiffening element model.

In this paper, the joint stiffening element is an improved beam element that can compensate for the joint stiffening effect. It also has a much lower computational cost than the solid element model. It can accelerate the design process of lattice structures. It can also give designers more accurate results when simulating the mechanical performance of lattice structures.

Table 3 The comparison of the computational costs between the solid element model and the proposed model

	Cubic-center			Vintiles		
	Element	DOFs	Time(s)	Element	DOFs	Time(s)
3D element (coarse)	369440	393087	61	252149	275109	36
3D element (fine)	15529031	11057385	3397	15486480	10719162	3686
Proposed model	2040	2796	0.25	4356	14724	0.56

5. Conclusions

In this paper, a concept called joint stiffening element is proposed to investigate the influence of the joint on the stiffness property of lattice structures. The joint stiffening element is divided into three segments. The segments at two ends represent the joint area in the lattice strut. The middle segment represents the actual strut length of the lattice structure. Four parameters are

defined in the proposed element to evaluate the stiffening effect of the joint on a single lattice strut. Then, the stiffness matrix of the proposed element is derived by rearranging the displacement vector and the load vector. A parametric study has been conducted to determine the optimal parameters of the joint stiffening element for a specific lattice structure. The unit axial load and transverse load are added on the lattice strut to investigate the influence of the joint on the tensile and flexural properties.

To validate the proposed model, the lattice structures with Cubic-center and Vintiles topologies have been fabricated for the three-point-bend testing. Tensile specimens are tested to obtain the as-fabricated material property in order to reduce the influence caused by the manufacturing process. It is found that the elastic modulus of the vertical strut is 20% lower than that of the horizontal strut and inclined strut. The lattice structure is simulated using the beam element model, the solid element model, the proposed model, and the models in literature. It is found that the influence of the joint is more obvious on the bending dominant topology than the stretching dominant topology. For the Vintiles lattice structure, the stiffness predicted by the beam element model is only 52.7% of the experimental result. However, the proposed model that considers the joint influence can accurately estimate the stiffness of the structure. For the Cubic-center lattice structure, the difference between the result of the beam element model and the experimental result is only 12.5%. This is because most struts in Cubic-center lattice structure are under axial load instead of bending load, in which case the joint stiffening effect is not that significant. Nevertheless, the result obtained by the proposed model is still closer to the experimental result than the traditional beam element model. Future research will focus on the feasibility of the joint stiffening element on the heterogeneous lattice structures. Because the joint size is nonuniform in heterogeneous lattice structures, a relationship between the parameter and the joint size should be established. The application of the joint stiffening element in the nonlinear analysis will also be investigated to simulate the plastic deformation of lattice structures.

Acknowledgment

This research work is supported by National Sciences and Engineering Research Council of Canada Discovery Grant RGPIN436055-2013.

Reference

[1] G. Dong, Y. Tang, and Y. F. Zhao, "A Survey of Modeling of Lattice Structures Fabricated by Additive Manufacturing," *Journal of Mechanical Design,* vol. 139, no. 10, pp. 100906-100906-13, 2017.

[2] Y. Tang, G. Dong, Q. Zhou, and Y. F. Zhao, "Lattice Structure Design and Optimization With Additive Manufacturing Constraints," *IEEE Transactions on Automation Science and Engineering,* vol. PP, no. 99, pp. 1-17, 2017.

[3] M. Alzahrani, S. K. Choi, and D. W. Rosen, "Design of truss-like cellular structures using relative density mapping method," *Materials and Design,* Article vol. 85, pp. 349-360, 2015.

[4] T. Tancogne-Dejean, A. B. Spierings, and D. Mohr, "Additively-manufactured metallic micro-lattice materials for high specific energy absorption under static and dynamic loading," *Acta Materialia,* Article vol. 116, pp. 14-28, 2016.

[5] H. Brooks and K. Brigden, "Design of conformal cooling layers with self-supporting lattices for additively manufactured tooling," *Additive Manufacturing,* Article vol. 11, pp. 16-22, 2016.

[6] L. Gibson, M. Ashby, G. Schajer, and C. Robertson, "The mechanics of two-dimensional cellular materials," in *Proceedings of the Royal Society of London A: Mathematical, Physical and Engineering Sciences*, 1982, vol. 382, no. 1782, pp. 25-42: The Royal Society.

[7] L. J. Gibson and M. F. Ashby, "The mechanics of three-dimensional cellular materials," in *Proceedings of the Royal Society of London A: Mathematical, Physical and Engineering Sciences*, 1982, vol. 382, no. 1782, pp. 43-59: The Royal Society.

[8] G. N. Labeas and M. M. Sunaric, "Investigation on the Static Response and Failure Process of Metallic Open Lattice Cellular Structures," *Strain,* vol. 46, no. 2, pp. 195-204, 2010.

[9] H. Alsalla, L. Hao, and C. Smith, "Fracture toughness and tensile strength of 316L stainless steel cellular lattice structures manufactured using the selective laser melting technique," *Materials Science and Engineering: A,* vol. 669, pp. 1-6, 7/4/ 2016.

[10] L. Yang, D. Cormier, H. West, O. Harrysson, and K. Knowlson, "Non-stochastic Ti-6Al-4V foam structures with negative Poisson's ratio," (in English), *Materials Science and Engineering A,* Article vol. 558, pp. 579-585, 2012.

[11] R. E. Winter *et al.*, "Plate-impact loading of cellular structures formed by selective laser melting," *Modelling and Simulation in Materials Science and Engineering,* Article vol. 22, no. 2, 2014, Art. no. 025021.

[12] A. Salehian and D. J. Inman, "Dynamic analysis of a lattice structure by homogenization: Experimental validation," *Journal of Sound and Vibration,* vol. 316, no. 1–5, pp. 180-197, 9/23/ 2008.

[13] M. Jamshidinia, L. Wang, W. Tong, R. Ajlouni, and R. Kovacevic, "Fatigue properties of a dental implant produced by electron beam melting (EBM)," *Journal of Materials Processing Technology,* Article vol. 226, pp. 255-263, 2015.

[14] S. I. Park, D. W. Rosen, S. K. Choi, and C. E. Duty, "Effective mechanical properties of lattice material fabricated by material extrusion additive manufacturing," (in English), *Additive Manufacturing,* Article vol. 1, pp. 12-23, 2014.

[15] S. Cahill, S. Lohfeld, and P. McHugh, "Finite element predictions compared to experimental results for the effective modulus of bone tissue engineering scaffolds fabricated by selective laser sintering," *Journal of Materials Science: Materials in Medicine,* vol. 20, no. 6, pp. 1255-1262, 2009.

[16] L. Yang, O. Harrysson, H. West, and D. Cormier, "Mechanical properties of 3D re-entrant honeycomb auxetic structures realized via additive manufacturing," *International Journal of Solids and Structures,* Article in Press 2015.

[17] M. R. Karamooz Ravari, M. Kadkhodaei, M. Badrossamay, and R. Rezaei, "Numerical investigation on mechanical properties of cellular lattice structures fabricated by fused deposition modeling," *International Journal of Mechanical Sciences,* Article vol. 88, pp. 154-161, 2014.

[18] G. Campoli, M. S. Borleffs, S. Amin Yavari, R. Wauthle, H. Weinans, and A. A. Zadpoor, "Mechanical properties of open-cell metallic biomaterials manufactured using additive manufacturing," *Materials & Design,* vol. 49, pp. 957-965, 8// 2013.

[19] M. Suard, P. Lhuissier, R. Dendievel, J. J. Blandin, F. Vignat, and F. Villeneuve, "Towards stiffness prediction of cellular structures made by electron beam melting (EBM)," *Powder Metallurgy,* Article vol. 57, no. 3, pp. 190-195, 2014.

[20] T. B. Sercombe *et al.*, "Failure modes in high strength and stiffness to weight scaffolds produced by Selective Laser Melting," *Materials and Design,* Article vol. 67, pp. 501-508, 2015.
[21] M. Smith, Z. Guan, and W. J. Cantwell, "Finite element modelling of the compressive response of lattice structures manufactured using the selective laser melting technique," *International Journal of Mechanical Sciences,* vol. 67, pp. 28-41, 2// 2013.
[22] M. H. Luxner, J. Stampfl, and H. E. Pettermann, "Finite element modeling concepts and linear analyses of 3D regular open cell structures," *Journal of Materials Science,* Conference Paper vol. 40, no. 22, pp. 5859-5866, 2005.
[23] D. W. R. Sang-in Park, "Homogenization of Mechanical Properties for Additively Manufactured Periodic Lattice Structures Considering Joint Stiffening Effects," presented at the IDETC/CIE, Charlotte, North Carolina, 2016.
[24] C. Díaz, M. Victoria, O. M. Querin, and P. Martí, "Optimum design of semi-rigid connections using metamodels," *Journal of Constructional Steel Research,* vol. 78, pp. 97-106, 2012.
[25] J. N. Reddy, *An introduction to the finite element method* (no. 2.2). 1993.
[26] K.-J. Bathe, *Finite element procedures*. Klaus-Jurgen Bathe, 2006.
[27] Z.-Q. Qu, *Model order reduction techniques with applications in finite element analysis*. Springer Science & Business Media, 2013.
[28] ASTM D638-14, Standard Test Method for Tensile Properties of Plastics, ASTM International, West Conshohocken, PA, 2014, www.astm.org.
[29] ASTM D790-17, Standard Test Methods for Flexural Properties of Unreinforced and Reinforced Plastics and Electrical Insulating Materials, ASTM International, West Conshohocken, PA, 2017, www.astm.org.